Syntheses, Crystal Structures and Properties of Two New Manganese(II) Coordination Polymers with Tetrafluorophthalate Ligands

Sheng-Chun Chen[a,b], Jing Qin[a], Zhi-Hui Zhang[a], Xiao-Xiao Cai[a], Jian Gao[b], Li Liu[a], Ming-Yang He[a], and Qun Chen[a]

[a] Key Laboratory of Fine Petro-chemical Technology, Changzhou University, Changzhou 213164, People's Republic of China

[b] School of Chemical Engineering, Nanjing University of Science & Technology, Nanjing 210094, People's Republic of China

Reprint requests to Prof. Q. Chen and Prof. M.-Y. He. Fax: +8651986330251.
E-mail: chenqunjpu@yahoo.com (Q. Chen), hemingyangjpu@yahoo.com (M.-Y. He)

Z. Naturforsch. **2013**, *68b*, 277 – 283 / DOI: 10.5560/ZNB.2013-3022
Received January 22, 2013

Two new polymeric Mn^{II} complexes, $\{[Mn(1,2\text{-BDC-}F_4)(H_2O)_3](EtOH)\}_n$ (**1**) and $[Mn(1,2\text{-BDC-}F_4)(H_2O)_2(DMF)]_n$ (**2**), have been prepared from the reaction of Mn^{II} acetate with 3,4,5,6-tetrafluoro-benzene-1,2-dicarboxylic acid (1,2-H_2BDC-F_4) using different solvents, and characterized by elemental analysis, IR spectroscopy, thermogravimetric (TG) analysis, and single-crystal X-ray structure analysis. Both complexes crystallize in the triclinic space group $P\bar{1}$ and have similar one-dimensional double chain structures, consisting of a unique arrangement of 8-membered and 14-membered rings. The effects of solvent as ligand and/or guest on the self-assembly processes of the supramolecular networks and on their photoluminescence properties in the solid state are discussed.

Key words: Coordination Polymer, Solvent-induced Synthesis, Mn^{II} Tetrafluorophthalate, Crystal Structure, Luminescence Properties

Introduction

In the past decade, the design and synthesis of coordination polymers involving transition metal ions and organic ligands have become one of the most active research fields in coordination chemistry and crystal engineering for achieving new materials [1 – 3]. Suitable organic ligands favoring structure-specific self-assembly are the basis for the construction of coordination architectures. In this respect, aromatic dicarboxylate ligands [for example, benzene-1,*n*-dicarboxylates (1,*n*-BDC, $n = 2$, 3, and 4)] [4 – 11] and their substituted derivatives [12 – 17], which exhibit diverse coordination modes, have been widely used in the preparation of various polymeric metal carboxylates. It is well-known that electron-donating or -withdrawing groups on the aromatic backbone can significantly affect the formation of crystalline networks and result in different coordination polymers with unique physicochemical properties [18]. In this context, fluorous molecules are of particular interest, and fluorinated bridging benzenedicarboxylate ligands such as 2,3,5,6-tetrafluoro-benzene-1,4-dicarboxylate [19 – 21], 2,4,5,6-tetrafluoro-benzene-1,3-dicarboxylate [22, 23] and 5-fluoro-benzene-1,3-dicarboxylate [24], have been employed to build extended networks with metal ions. Advantages mainly result from the following two factors: the first is the significant enhancement of acidity because of the strong electron-withdrawing effect of fluorine substituents, which can lead to the complete deprotonation of the carboxylic group upon its reaction with metal ions. The second is the steric hindrance effect that the fluorine atoms have on the torsion angle by which the carboxylate groups are twisted out of the plane of the benzene ring. Moreover, host-guest C–H···F and O–H···F contacts can be as important as C–H···O/C–H···N and O–H···O/O–H···N interactions in stabilizing a specific structure [25, 26], and can be applied in crystal design. Encouraged by all that was mentioned above, we have chosen 3,4,5,6-tetrafluoro-benzene-1,2-dicarboxylic acid (1,2-

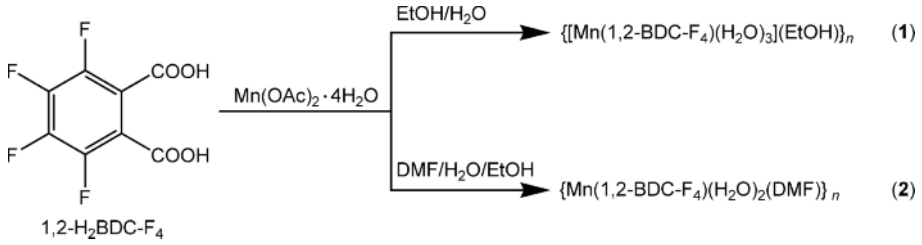

Scheme 1.

H_2BDC-F_4) to construct Ag^I and Cd^{II} coordination architectures exhibiting interesting antibacterial activity and luminescence properties [27, 28]. As a continuation of our work, herein, we wish to report the solvent-regulated self-assembly of two new Mn^{II} tetrafluorophthalate coordination polymers {[Mn(1,2-BDC-F_4)(H_2O)$_3$](EtOH)}$_n$ (**1**) and {Mn(1,2-BDC-F_4)(H_2O)$_2$(DMF)}$_n$ (**2**) (Scheme 1). In addition, the spectroscopic, thermal and luminescence properties of both complexes are presented and discussed.

Results and Discussion

Synthesis and general characterization

It is well-known that the selection of solvent systems plays an important role in governing coordination arrays and the final supramolecular architectures. Among the widely used organic solvents, DMF was proved to be a reliable binding guest molecule participating in coordination networks of Mn^{II} and Cu^{II} ions [29, 30]. Its coordinating ability is better than that of EtOH, MeOH and the aqua ligand in mixed solvent media. In this study, we choose 1,2-H_2BDC-F_4 as a rigid bridging ligand to synthesize Mn^{II} coordination polymers in two different solvent mixtures, namely, EtOH-H_2O and EtOH-H_2O-DMF. The two Mn^{II} complexes could be isolated independent of the counteranions through the same procedure when alternating the starting metal salts using $Mn(OAc)_2$, $MnCl_2$ or $Mn(ClO_4)_2$. Both complexes are stable under ambient conditions and insoluble in water and common organic solvents, which is consistent with their polymeric nature. In the IR spectra, the broad bands centered in the 3500 – 3000 cm^{-1} region indicate the O–H stretching of the solvents. The absence of characteristic absorption bands at ~1740 and ~1715 cm^{-1} of the carboxyl moiety in **1** and **2** suggests complete deprotonation. As a result, the antisymmetric and symmetric carboxylate stretching vibrations are found in the range of 1605 – 1615 and 1390 – 1440 cm^{-1}, respectively.

*Crystal structures of **1** and **2***

X-Ray diffraction analysis revealed that complexes **1** and **2** crystallize in the triclinic space group $P\bar{1}$ and have chain structures. The basic coordination frameworks of **1** and **2** are similar and consist of double chains of the composition [Mn(1,2-BDC-F_4)]$_n$, except that the coordinated guest molecules are H_2O in **1** and H_2O and DMF in **2**. So, only the molecular structure of **1** will be described in more detail. The asymmetric unit of **1** contains one Mn^{II} ion, one 1,2-BDC-F_4 dianion, three H_2O ligands, as well as one non- coordinated EtOH molecule. As shown in Fig. 1, the octahedral environment of the Mn^{II} center is provided by three carboxylate oxygen atoms (O1, O3#1 and O4#2) from three 1,2-BDC-F_4 dianions and three oxygen atoms (O5, O6, and O7) from three terminal H_2O molecules with the Mn–O distances in the range of 2.115(2) – 2.238(2) Å. The O–Mn–O bond angles vary from 85.6(1) to 177.5(1)° (see Table 1 for detailed bond parameters). Each 1,2-BDC-F_4 ligand adopts a μ_3-bridging fashion with one carboxylate group in a μ_2-$\eta^1:\eta^1$-bridging mode and the other one in a μ_1-$\eta^1:\eta^0$-monodentate mode to connect with three Mn^{II} ions to generate a double chain featuring a unique alternating arrangement of 8-membered and 14-membered rings (Fig. 1). The successive Mn···Mn separations are 4.690 and 6.598 Å, respectively. It should be noted that such an arrangement of a double chain is different from that of the reported Mn^{II} and Cu^{II} *ortho*-phthalate complexes [31, 32], where one carboxylate group shows complete deprotonation, and the other one is assigned to the monodeprotonation fashion, thus forming a double chain possessing a continuous arrangement of 14-membered rings.

Table 1. Selected bond lengths (Å) and angles (deg) for **1** and **2** with estimated standard deviations in parentheses[a].

1		**2**	
Bond lengths		Bond lengths	
Mn1–O1	2.150(2)	Mn1–O1	2.130(3)
Mn1–O3#1	2.204(2)	Mn1–O3#3	2.221(3)
Mn1–O4#2	2.115(2)	Mn1–O4#4	2.147(3)
Mn1–O5	2.195(2)	Mn1–O5	2.236(3)
Mn1–O6	2.197(2)	Mn1–O6	2.180(3)
Mn1–O7	2.238(2)	Mn1–O7	2.175(3)
Bond angles		Bond angles	
O1–Mn1–O3#2	91.5(1)	O1–Mn1–O3#3	90.4(1)
O1–Mn1–O4#2	166.6(1)	O1–Mn1–O4#4	171.2(1)
O1–Mn1–O5	85.0(1)	O1–Mn1–O5	85.2(1)
O1–Mn1–O6	97.3(1)	O1–Mn1–O6	99.6(1)
O1–Mn1–O7	79.5(1)	O1–Mn1–O7	85.1(1)
O3#1–Mn1–O4#2	101.8(1)	O3#3–Mn1–O4#4	98.1(1)
O3#1–Mn1–O5	93.5(1)	O3#3–Mn1–O5	169.9(1)
O3#1–Mn1–O6	85.6 (1)	O3#3–Mn1–O6	83.8(1)
O3#1–Mn1–O7	168.6 (1)	O3#3–Mn1–O7	89.9(1)
O4#2–Mn1–O5	93.6(1)	O4#4–Mn1–O5	86.7(1)
O4#2–Mn1–O6	84.3(1)	O4#4–Mn1–O6	83.6(1)
O4#2–Mn1–O7	87.1(1)	O4#4–Mn1–O7	92.7(1)
O5–Mn1–O6	177.5(1)	O5–Mn1–O6	89.0(1)
O5–Mn1–O7	92.7(1)	O5–Mn1–O7	98.8(1)
O6–Mn1–O7	88.4(1)	O6–Mn1–O7	172.1(1)

[a] Symmetry codes. For **1**, #1: $-x+1, -y+1, -z+1$; #2: $x+1, y+1, z$; for **2**, #3: $-x+1, -y+1, -z$; #4: $x-1, y+1, z$.

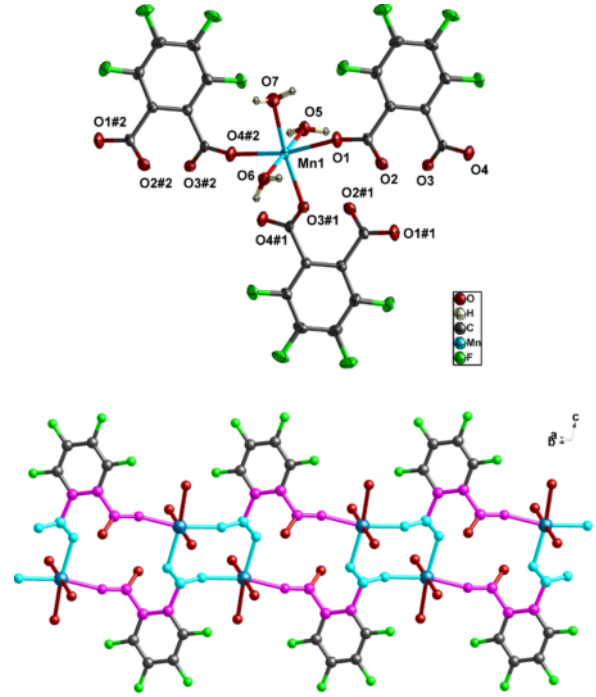

Fig. 1 (color online). Views of: (top) the coordination environment of the Mn^{II} center in **1** (for symmetry codes see Table 1), and (bottom) the polymeric double chain of **1**, highlighting the alternating arrangement of 8- and 14-membered rings by turquoise and pink bonds, respectively.

Although both **1** and **2** show a similar 1-D coordination array, the introduction of DMF into the solvent leads to a change of the solvate molecule and formation of a different supramolecular framework for **2**. There exist diverse hydrogen bonding motifs in the crystal structure of **1**. Strong intramolecular O7–H7A···F1 interactions (see Table 2 for details of hydrogen bonding) have been found to stabilize the double-chain motifs. With respect to the EtOH molecule, it works as a linker to fabricate a supramolecular layer by connecting two neighboring parallel coordination chains through intermolecular O–H···O hydrogen bonds (O7–H7B···O8 and O8–H8···O5, see Table 2) with the coordinated H_2O ligands, as illustrated in Fig. 2. However, in **2**, these adjacent 1-D arrays are connected through strong direct O–H···O hydrogen bonding interactions

Table 2. Hydrogen bonding geometries in the crystal structures of **1** and **2**.

Complex	D–H···A	H···A (Å)	D···A (Å)	D–H···A (deg)	Symmetry code
1	O5–H5A···O2	1.95	2.751(3)	167	$x, y+1, z$
	O5–H5B···O6	2.07	2.881(3)	170	$x-1, y, z$
	O6–H6A···O3	2.00	2.771(3)	156	$x+1, y, z$
	O6–H6B···O2	1.83	2.640(3)	168	$-x+2, -y+1, -z+1$
	O7–H7A···F1	2.16	2.981(3)	178	
	O7–H7B···O8	1.92	2.721(5)	166	$x+1, y, z$
	O8–H8···O5	2.16	2.883(4)	146	
2	O6–H6A···O2	1.81	2.654(4)	174	$-x, -y+1, -z$
	O6–H6B···O3	1.93	2.750(4)	161	$x-1, y, z$
	O7–H7A···O2	1.87	2.711(4)	171	$x, y+1, z$
	O7–H7B···O6	2.21	3.018(4)	160	$x+1, y, z$
	C9–H9···O7	2.48	3.402(6)	169	$x-1, y, z$

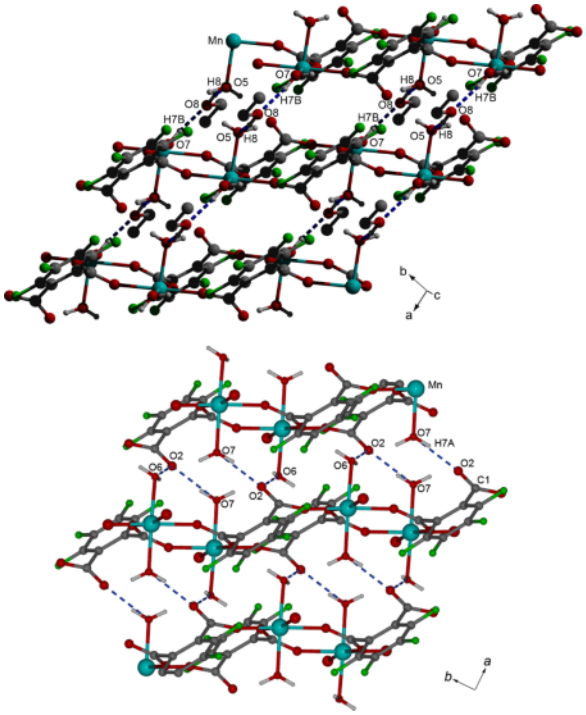

Fig. 2 (color online). Views of: (top) the supramolecular layer structure in **1** constructed *via* O–H···O interactions (blue dashed lines) between the coordination chains, and (bottom) the supramolecular layer structure in **2**, showing the direct O–H···O hydrogen interactions (blue dashed lines) between the coordination chains.

(see Table 2 for details of hydrogen bonding) to afford a supramolecular layer array (Fig. 2).

*Thermal stability of **1** and **2***

Thermogravimetric analyses (TG) were carried out for complexes **1** and **2** (Fig. 3). In the case of **1**, the weight loss of 24.7 % occurring from 45 to *ca.* 235 °C corresponds to the removal of the coordinated aqua ligands and ethanol guests (calcd. 25.6 %). Then, a sharp weight loss occurs with an onset temperature of *ca.* 360 °C for degradation of the residual fragment, followed by continuous slow weight loss up to 800 °C. Complex **2** is stable up to 150 °C and displays two consecutive steps of weight loss below 260 °C, indicating the elimination of coordinated H_2O and DMF molecules (observed: 26.3 %; calcd. 27.2 %). Subsequently, pyrolysis of the residual coordination framework is observed and further heating to 800 °C reveals a gradual weight loss of the sample.

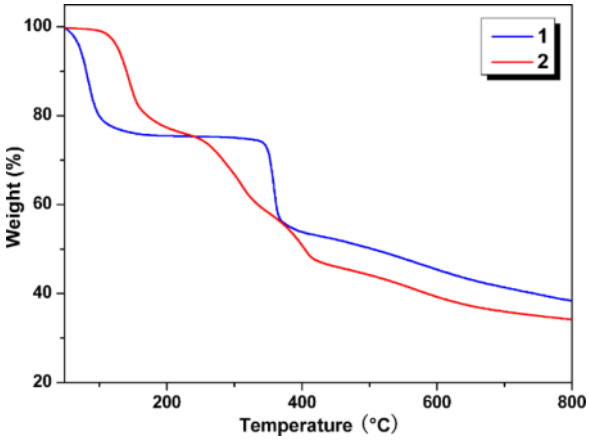

Fig. 3 (color online). TGA curves of complexes **1** and **2**.

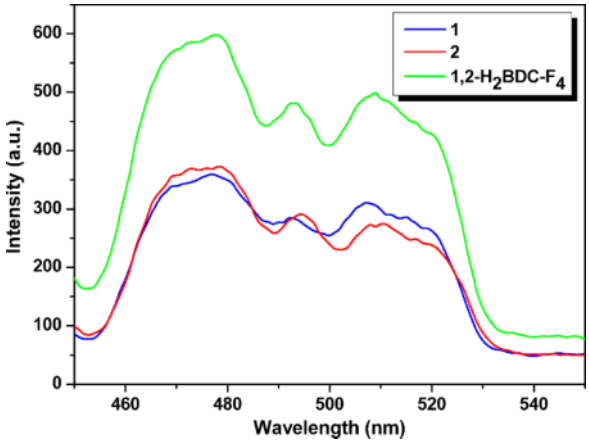

Fig. 4 (color online). Solid-state fluorescence emission spectra of complexes **1**, **2** and the free ligand 1,2-H_2BDC-F_4.

*Photoluminescence properties of **1** and **2***

The emission spectra of complexes **1** and **2** as well as of the organic ligand 1,2-H_2BDC-F_4 were investigated in the solid state at room temperature (Fig. 4). Upon excitation at 336 nm, the free ligand exhibits the maximum fluorescence emission band centered at 478 nm, which can be ascribed to the $\pi \rightarrow \pi^*$ and/or $n \rightarrow \pi^*$ transitions. For complexes **1** and **2**, the maximum emission bands are similarly observed at 477 nm for **1** and 479 nm for **2** ($\lambda_{ex} = 336$ nm), and are tentatively attributed to ligand-centered transitions. Furthermore, the emission intensities of **1** and **2** are significantly weaker than that of the free ligand, which is likely related to their complicated struc-

Table 3. Crystal structure data for **1** and **2**.

	1	**2**
Formula	$C_{10}H_{12}F_4MnO_8$	$C_{11}H_{11}F_4MnNO_7$
M_r	391.14	400.15
Crystal size, mm^3	$0.24 \times 0.22 \times 0.20$	$0.24 \times 0.20 \times 0.18$
Crystal system	triclinic	triclinic
Space group	$P\bar{1}$	$P\bar{1}$
a, Å	6.148(1)	6.218(1)
b, Å	7.613(1)	7.605(1)
c, Å	15.720(2)	15.562(3)
α, deg	100.142(2)	84.365(4)
β, deg	92.918(2)	89.384(4)
γ, deg	98.723(3)	81.325(4)
V, Å^3	713.6(2)	723.9(3)
Z	2	2
$D_{calcd.}$, g cm^{-3}	1.82	1.84
μ(Mo K_α), cm^{-1}	1.0	1.0
F(000), e	394	402
hkl range	$-7 \le h \le +7$	$-7 \le h \le +6$
	$-6 \le k \le +9$	$-7 \le k \le +9$
	$-19 \le l \le +19$	$-18 \le l \le +18$
Refl. measured / unique / R_{int}	4294 / 2764 / 0.0207	3877 / 2506 / 0.0193
Param. refined	210	219
$R1$[a] / $wR2$[b] (all data)	0.0390 / 0.1410	0.0638 / 0.2046
GoF (F^2)[c]	1.029	1.053
$\Delta\rho_{fin}$ (max / min), e Å^{-3}	0.50 / −0.79	0.94 / −1.08

[a] $R1 = \Sigma||F_o| - |F_c||/\Sigma|F_o|$; [b] $wR2 = [\Sigma w(F_o^2 - F_c^2)^2/\Sigma w(F_o^2)^2]^{1/2}$, $w = [\sigma^2(F_o^2) + (AP)^2 + BP]^{-1}$, where $P = (\mathrm{Max}(F_o^2, 0) + 2F_c^2)/3$; [c] $\mathrm{GoF} = [\Sigma w(F_o^2 - F_c^2)^2/(n_{obs} - n_{param})]^{1/2}$.

tures as well as the decay effect of high-energy C–H and/or O–H oscillators of lattice and coordinated solvent molecules [33].

Conclusion

In summary, solvent-regulated assemblies of the Mn^{II} ion with the perfluorinated phthalate ligand 1,2-BDC-F_4 lead to the formation of two new coordination polymers. The solvent media used in the preparations play a significant role in the buiding of the final host-guest supramolecular networks that are co-stabilized by intermolecular O–H···F hydrogen bonding interactions. These results will prompt us to make a further systematic study on the coordination chemistry of fluorinated aromatic carboxylate ligands, which will enrich the scope of crystal engineering for supramolecular hybrid solids.

Experimental Section

All reagents and solvents were commercially available and used without further purification. Infrared spectra were recorded with a Nicolet ESP 460 FT-IR spectrometer on KBr pellets in the range of 4000 – 400 cm^{-1}. Elemental analyses were performed with a PE-2400II (Perkin-Elmer) elemental analyzer. Thermogravimetric analysis (TGA) experiments were carried on a Dupont thermal analyzer from room temperature to 800 °C (heating rate of 10 °C min^{-1}, nitrogen stream). Fluorescence spectra of the solid samples were recorded with a Varian Cary Eclipse spectrometer at room temperature.

*Synthesis of {[Mn(1,2-BDC-F_4)(H_2O)$_3$](EtOH)}$_n$ (**1**)*

In a 25 mL vial, a mixture of $Mn(OAc)_2{\cdot}4H_2O$ (300 mg, 1.2 mmol) and 1,2-H_2BDC-F_4 (288 mg, 1.2 mmol) was dissolved in EtOH-H_2O (3 : 1, v : v; 18.0 mL) with stirring for *ca.* 30 min. The resulting solution was filtered and left to stand at room temperature. Colorless block-shaped crystals of **1** suitable for X-ray diffraction were obtained by slow evaporation of the filtrate in 52 % yield (244 mg, on the basis of 1,2-H_2BDC-F_4). – Anal. for $C_{10}H_{12}F_4MnO_8$ (%): calcd. C 30.71, H 3.09; found C 30.63, H 3.11. – IR (KBr pellet): ν = 3261.7 bs, 2978.5 m, 2927.2 m, 1608.3 vs, 1516.4 s, 1466.7 s, 1425.0 s, 1392.8 vs, 1282.1 m, 1188.6 m, 1072.3 w, 1044.5 w, 949.6 s, 762.6 m cm^{-1}.

*Synthesis of [Mn(1,2-BDC-F_4)(H_2O)$_2$(DMF)]$_n$ (**2**)*

The procedure was the same as that for **1** except that DMF (4.5 mL) was added to the mixted solvent EtOH-H_2O, giv-

ing colorless block-shaped crystals of **2** upon slow evaporation after one week in 78 % yield (375 mg, on the basis of 1,2-H_2BDC-F_4). – Anal. for $C_{11}H_{11}F_4MnNO_7$ (%): calcd. C 33.02, H 2.77, N 3.50; found C 32.86, H 2.78, N 3.54. – IR (KBr pellet): $\nu = 3229.2$ bs, 2965.8 m, 2936.4 m, 1612.6 vs, 1509.5 s, 1465.6 s, 1425.4 s, 1390.2 vs, 1119.4 s, 1101.9 m, 1064.4 w, 949.7 s, 832.2 m, 761.4 m, 703.8 m cm^{-1}.

Crystal structure determinations

Single-crystal X-ray diffraction data for complexes **1** and **2** were collected on a Bruker Apex II CCD diffractometer with MoK_α radiation ($\lambda = 0.71073$ Å) at room temperature. A semiempirical absorption correction was applied (SADABS [34]), and the program SAINT was used for integration of the diffraction profiles [35]. The structures were solved by Direct Methods using SHELXS and refined by full-matrix least-squares calculations on F^2 using SHELXL [36 – 39]. All non-hydrogen atoms were refined anisotropically. C-bound H atoms were placed in geometrically calculated positions and refined using a riding model. O-bound H atoms were localized by difference Fourier maps and refined in subsequent refinement cycles. Further crystallographic details are summarized in Table 3, and selected bond lengths and angles are listed in Table 1.

CCDC 920052 and 920053 contain the supplementary crystallographic data for this paper. These data can be obtained free of charge from The Cambridge Crystallographic Data Centre *via* www.ccdc.cam.ac.uk/data_request/cif.

Acknowledgement

We gratefully acknowledge the financial support from the National Natural Science Foundation of China (21201026), and from the Priority Academic Program Development of Jiangsu Higher Education Institutions (PAPD) as well as from the Open Foundation of Jiangsu Province Key Laboratory of Fine Petrochemical Technology (KF1005).

[1] J. J. Perry, J. A. Perman, M. J. Zaworotko, *Chem. Soc. Rev.* **2009**, *38*, 1400 – 1417.
[2] D. J. Tranchemontagne, J. L. Mendoza-Cortés, M. O'Keeffe, O. M. Yaghi, *Chem. Soc. Rev.* **2009**, *38*, 1257 – 1283.
[3] N. W. Ockwing, O. Delgado-Friedrichs, M. O'Keeffe, O. M. Yaghi, *Acc. Chem. Res.* **2005**, *38*, 176 – 182.
[4] N. L. Rosi, J. Kim, M. Eddaoudi, B. L. Chen, M. O'Keeffe, O. M. Yaghi, *J. Am. Chem. Soc.* **2005**, *127*, 1504 – 1518.
[5] J. Sun, Y. Zhou, Q. Fang, Z. Chen, L. Weng, G. Zhu, S. Qiu, D. Zhao, *Inorg. Chem.* **2006**, *45*, 8677 – 8684.
[6] A. L. Grzesiak, F. J. Uribe, N. W. Ockwig, O. M. Yaghi, A. J. Matzger, *Angew. Chem. Int. Ed.* **2006**, *45*, 2553 – 2556.
[7] B. Moulton, H. Abourahma, M. W. Bradner, J. Lu, G. J. McManus, M. J. Zaworotko, *Chem. Commun.* **2003**, *12*, 1342 – 1343.
[8] C. Livage, N. Guillou, J. Chaigneau, P. Rabu, M. Drillon, G. Férey, *Angew. Chem. Int. Ed.* **2005**, *44*, 6488 – 6491.
[9] D.-X. Hu, F. Luo, Y.-X. Che, J.-M. Zheng, *Cryst. Growth Des.* **2007**, *7*, 1733 – 1737.
[10] M. Du, X.-J. Jiang, X.-J. Zhao, *Inorg. Chem.* **2007**, *46*, 3984 – 3995.
[11] Y. Qi, F. Luo, Y. Che, J. Zheng, *Cryst. Growth Des.* **2008**, *8*, 606 – 611.
[12] T.-P. Hu, H.-Y. He, F.-N. Dai, X.-L. Zhao, D.-F. Sun, *CrystEngComm* **2010**, *12*, 2018 – 2020.
[13] X.-P. Zhou, Z.-T. Xu, M. Zeller, A.-D. Hunter, S. S.-Y. Chui, C.-M. Chen, *Inorg. Chem.* **2008**, *47*, 7459 – 7461.
[14] L.-X. Shi, C.-D. Wu, *Inorg. Chem. Commun.* **2011**, *14*, 569 – 572.
[15] P. D. C. Dietzel, R. E. Johnsen, H. Fjellvåg, S. Bordiga, E. Groppo, S. Chavan, R. Blom, *Chem. Commun.* **2008**, *41*, 5125 – 5127.
[16] J. He, Z.-T. Yang, M. Zeller, A. D. Hunter, J.-H. Lin, *J. Solid State Chem.* **2009**, *182*, 1821 – 1826.
[17] S.-C. Chen, Z.-H. Zhang, Y.-S. Zhou, W.-Y. Zhou, Y.-Z. Li, M.-Y. He, Q. Chen, M. Du, *Cryst. Growth Des.* **2011**, *11*, 4190 – 4197.
[18] J. L. C. Rowsell, O. M. Yaghi, *J. Am. Chem. Soc.* **2006**, *128*, 1304 – 1315.
[19] C. Seidel, R. Ahlers, U. Ruschewitz, *Cryst. Growth. Des.* **2011**, *11*, 5053 – 5063.
[20] S.-C. Chen, Z.-H. Zhang, Q. Chen, H.-B. Bao, Q. Liu, M.-Y. He, M. Du, *Inorg. Chem. Commun.* **2009**, *12*, 835 – 838.
[21] B. Chen, Y. Yang, F. Zapata, G. Qian, Y. Luo, J. Zhang, E. B. Lobkovsky, *Inorg. Chem.* **2006**, *45*, 8882 – 8886.
[22] Z. Wang, V. C. Kravtsov, R. B. Walsh, M. J. Zaworotko, *Cryst. Growth Des.* **2007**, *7*, 1154 – 1162.
[23] Z. Hulvey, J. D. Furman, S. A. Turner, M. Tang, A. K. Cheetham, *Cryst. Growth Des.* **2010**, *10*, 2041 – 2043.
[24] S.-C. Chen, R.-R. Qin, Z.-H. Zhang, J. Qin, H.-B. Gao, F.-A. Sun, M.-Y. He, Q. Chen, *Inorg. Chim. Acta* **2012**, *390*, 61 – 69.
[25] V. R. Thalladi, H. C. Weiss, D. Blaser, R. Boese, A. Nangia, G. R. Desiraju, *J. Am. Chem. Soc.* **1998**, *120*, 8702 – 8710.

[26] A. J. Mountford, S. J. Lancaster, S. J. Coles, P. N. Horton, D. L. Hughes, M. B. Hursthouse, M. E. Light, *Inorg. Chem.* **2005**, *44*, 5921 – 5933.
[27] S.-C. Chen, Z.-H. Zhang, Q. Chen, L.-Q. Wang, J. Xu, M.-Y. He, M. Du, X.-P. Yang, R. A. Jones, *Chem. Commun.* **2013**, *49*, 1270 – 1272.
[28] S.-C. Chen, Z.-H. Zhang, M.-Y. He, H. Xu, Q. Chen, *Z. Anorg. Allg. Chem.* **2010**, *636*, 824 – 829.
[29] S.-C. Chen, Z.-H. Zhang, K.-L. Huang, Q. Chen, M.-Y. He, A.-J. Cui, C. Li, Q. Liu, M. Du, *Cryst. Growth Des.* **2008**, *8*, 3437 – 3445.
[30] M.-Y. He, S.-C. Chen, Z.-H. Zhang, K.-L. Huang, F.-H. Yin, Q. Chen, *Inorg. Chim. Acta* **2009**, *362*, 2569 – 2576.
[31] J. W. Bats, A. Kallel, H. Fuess, *Acta Crystallogr.* **1978**, *B34*, 1705 – 519.
[32] B. L. Rodrigues, M. D. D. Costa, N. G. Fernandes, *Acta Crystallogr.* **1999**, *C55*, 1997 – 2000.
[33] X. Shi, G. Zhu, X. Wang, G. Li, Q. Fang, G. Wu, G. Tian, M. Xue, X. Zhao, R. Wang, S. Qiu, *Cryst. Growth Des.* **2005**, *5*, 207 – 213.
[34] G. M. Sheldrick, SADABS, Program for Empirical Absorption Correction of Area Detector Data, University of Göttingen (Germany) **2002**.
[35] SAINT, Software Reference Manual, Bruker Analytical X-ray Instruments Inc., Madison, Wisconsin (USA) **1998**.
[36] G. M. Sheldrick, SHELXTL NT (version 5.1), Bruker Analytical X-ray Instruments Inc., Madison, Wisconsin (USA) **2001**.
[37] G. M. Sheldrick, SHELXS/L-97, Programs for Crystal Structure Determination, University of Göttingen, Göttingen (Germany) **1997**.
[38] G. M. Sheldrick, *Acta Crystallogr.* **1990**, *A46*, 467 – 473.
[39] G. M. Sheldrick, *Acta Crystallogr.* **2008**, *A64*, 112 – 122.